

Effect of Main Operating Parameters on Al₂O₃ Spheroidization by Radio Frequency Plasma System

Dai Zhen, Cao Yongge, Ma Chaoyang, Tang Fei, Zhang Jiantao, Wang Wenchao, Du Miaomiao, Long Jiaqi, Yuan Xuanyi

Beijing Key Laboratory of Opto-electronic Functional Materials & Micro-nano Devices, Renmin University of China, Beijing 100872, China

Abstract: Micro-fine spherical alumina (Al₂O₃) powders with mean diameters of 7, 30 and 75 μm have been synthesized by the SY119-30kW radio frequency induction plasma spheroidization system. The effect of main operating parameters on spheroidization process was investigated. The results show that different axial positions of the injection probe strongly influence the effectiveness of the spheroidization treatment and Z=12.9 cm is the best position for Al₂O₃ spheroidization process as it is the middle of coil center for this spheroidization system. The obtained powders with smooth surface exhibit fantastic sphericity and preferable density. The spheroidization efficiency of synthesized powders is almost 100% at feeding rate of 65 g/min with the chamber pressure of 0.079 MPa. In addition, the chamber pressure is also the vital factor that influences the fabrication process and it should be coordinated with the carrier gas flow rate. The phase compositions characterized by X-ray diffraction (XRD) shows the same results under different sheath gas (Ar or N₂) conditions. Furthermore, the purity of the fabricated powders is improved after high temperature spheroidization treatment.

Key words: RF induction plasma; Spheroidization; Al₂O₃ powders

Compared with conventional processes, plasma technology has so many advantages in high temperature material processing that inductively coupled plasma (ICP) have been widely used for both laboratory-scale studies and industrial applications, such as thermal sprays^[1], waste treatment^[2], and thermal plasma metallurgy. As a high energy density and high purity source, plasma has attracted more and more attention in the field of powder synthesizing since 1970 s^[3,4]. In recent years, much research has been done in the synthesis of nano-particles and powder spheroidization^[5-7]. Compared to other available methods such as sintering^[8], precipitation method, sol-gel method, nucleation and growth method^[9], thermal plasma processing is a more effective method of synthesizing high melting point spherical powders with high purity because of its advantages of high temperature flame (up to 10⁴ K) with a rapidly cooling system and the minimum

contamination^[10-12].

Alumina (Al₂O₃) has been an extremely promising material for a variety of applications including aerospace, shipbuilding industry, national defense systems and other industrial applications^[13,14] because of its unique performance characterized by high melting point (2324.15 K), high mechanical strength, outstanding corrosion resistance and thermal insulating properties^[15,16]. Moreover, with high resistivity and good insulation performance, Al₂O₃ has been also applied to the main parts of YGA laser crystal and the substrates of integrated circuit. It is also the wonderful thermal conductive filler for rubber plastic, especially the micro-fine spherical powders with high density^[17].

In the present work, micro-fine spherical alumina (Al₂O₃) powders with different mean diameters have been synthesized by the Radio Frequency (RF) plasma

Received date: February 02, 2016

Foundation item: National Natural Science Foundation of China, Youth Fund (51302311); National Natural Science Foundation of China (51272282)

Corresponding author: Yuan Xuanyi, Ph. D., Beijing Key Laboratory of Opto-electronic Functional Materials & Micro-nano Devices, Renmin University of China, Beijing 100872, P. R. China, Tel: 0086-10-82502773, E-mail: yuanxuanyi@ruc.edu.cn

Copyright © 2017, Northwest Institute for Nonferrous Metal Research. Published by Elsevier BV. All rights reserved.

spheroidization system. The interactions of the principal controlling spheroidization process parameters including injection probe position, powder feeding rate and reaction chamber pressure have been studied.

1 Experiment

The SY119-30kW induction plasma system (Model PL-35, Tekna Plasma System Inc., Canada) used in this work mainly consists of a water-cooled induction plasma torch, a 3 MHz radio frequency power supply system, a water-cooled stainless steel reactor, big vibrating screw feeder, gas feeding system and powder collection units. Irregular alumina raw powders with mean diameters of 7, 30 and 75 μm were used in the experiments.

During the induction plasma process, stable plasma was first generated using argon as the center and sheath gas with the flow rates of 15 and 60 L/min, respectively. Particles conveyed by carrier gas were axially injected into the plasma stream from the top of the plasma torch at a feeding rate of 5~280 g/min, and then got completely melted or evaporated at the relatively high temperature region. The rapidly cooled tail in large plasma volume could help rapid solidification for the formation of spherical powders under the action of surface tension of materials in the liquid state^[18,19]. The detailed processing parameters are given in Table 1.

Morphology of the particles and number percentage of spherical particles were characterized through the image analysis of photographs obtained by scanning electron microscopy (SEM, FEI, NOVA, NANOSEM, 450). Phase identification was performed via X-ray diffractometry (XRD, Bruker AXS, D8 ADVANCE A25-X1-1A32C4B, Germany). The purity of the product was demonstrated by XRF(1800, Shimadzu, Japan).

2 Results and Discussion

2.1 Morphologies and size analysis

In this work, different kinds of fine spherical powders with smooth surface are obtained. Fig.1 shows the scanning electron micrographs (SEM) of alumina powders before and after induction plasma treatment. It can be seen that the

average particle size of raw alumina powders is 75 μm (Fig.1a₁) and 30 μm (Fig.1b₁), and all the particles are stably aggregated with smaller rough powders. Fig.1a₂, 1b₂ show the RF plasma synthesized powders with power of 28 kW and the probe position of Z=12.9 cm. The process were carried out with pure argon as center gas (15 L/min), carrier gas (5 L/min) and sheath gas (60 L/min) at the same powder feeding rate of 65 g/min. The reaction chamber pressures were 0.079 MPa (a₂) and 0.078 MPa (b₂). The processed powders were collected at the bottom of the powder collection units.

As shown in Fig.1, irregular initial powder particles with rough surface a₁, b₁ are nearly all changed to spherical a₂, b₂. The results also clearly show that the spherical particles are well-distributed and there is no adhesion among the particles, which is good for the fluidity and fillability of powders.

Fig.2 shows the scanning electron micrographs (SEM) of alumina powders with mean size of 7 μm before (Fig.2a) and after (Fig.2b) induction plasma treatment. The powders were treated with the probe position of Z=12.5 cm, which is the most different condition from before. This process was also carried out with pure argon as center gas (15 L/min), carrier gas (5 L/min) and sheath gas (60 L/min), but with the different powder feeding rate of 35 g/min. The reaction chamber pressure was 0.071 MPa. The processed powders were also collected at the bottom of the powder collection units.

It can be found from Fig.2a that the irregular alumina precursor with rough surface is not homogenous in granularity and there are a large number very small particles deposited upon the surface of coarse powders. But Fig.2b shows that all the inhomogeneous irregular particles are changed into spherical with different particle sizes.

Both the results in Fig.1 and Fig.2 reveal the remarkable sphere formation; as a result, different micro size powders could be produced. Comparing Fig.2b with 1a₂ and 1b₂, it can be easily found out that processed powders with mean particle size of 7 μm (Fig.2b) are not well-distributed like (Fig.1a₂) and (Fig.1b₂), but they are seriously inhomogeneous. The particle size of treated powders keeps consistent with raw materials, that is to say the selection of raw materials has a strong influence on particle size and uniformity of the processed particles.

2.2 XRD and XRF analysis

Alumina is polycrystalline material and corundum ($\alpha\text{-Al}_2\text{O}_3$) has been the most widely used and known. A typical XRD pattern of alumina before and after plasma processing is shown in Fig.3. It shows that the initial powder is amorphous. The XRD patterns of processed powders exhibit the intensity peaks of α -alumina. The results also implies alumina powders have not been nitrogenized with nitrogen as sheath gas. We cost less nitrogen with higher heat conductivity, so it may be a better

Table 1 Typical operating parameters

Parameter	Value
Power input/kW	28
Center gas, argon/L min ⁻¹	15
Sheath gas, argon or nitrogen/L min ⁻¹	60
Carrier gas, argon/L min ⁻¹	1~10
Water pressure/ 6.89×10^{-3} MPa	>24
Reaction chamber pressure/ 6.89×10^{-3} MPa	7~18
Powder feed rate/g min ⁻¹	5~280
Locations of powder probe, Z/cm	10~12.9

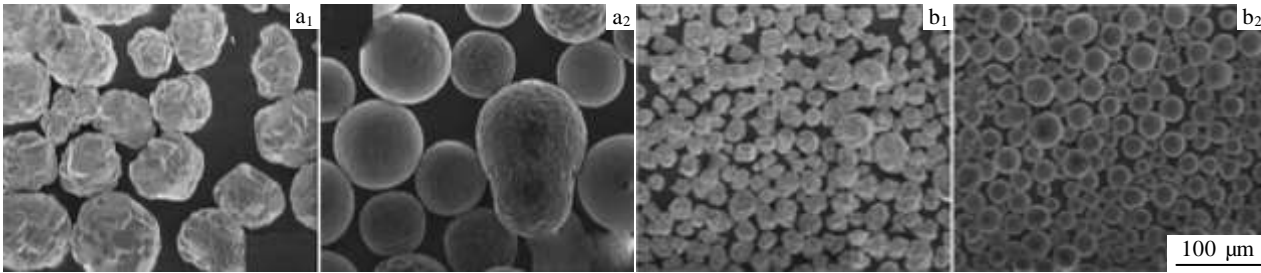


Fig.1 Morphologies of alumina powders with mean size of 75 μm (a_1 , a_2), 30 μm (b_1 , b_2) before (a_1 , b_1) and after (a_2 , b_2) plasma treatment (28 kW, $V=65$ g/min, $Z=12.9$ cm)

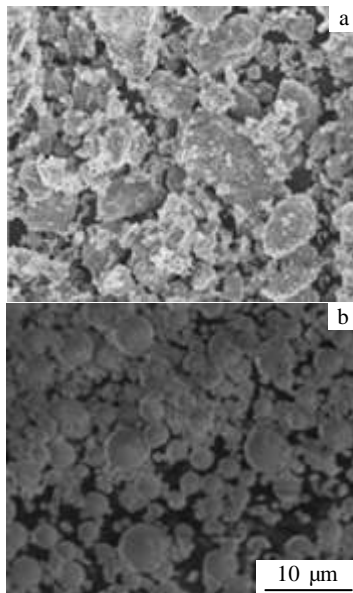


Fig.2 Morphologies of alumina powders with mean size of 7 μm before (a) and after (b) induction plasma treatment (25.8 kW, $V=35$ g/min, $Z=12.5$ cm)

choice as sheath gas. Because of the skin-effect, many powders are adsorbed to the internal wall of the reaction chamber. Fig.3 shows the powders got from the internal wall of the reaction chamber have the same results of the powders got from the bottom. It also shows that the reaction environment is so clean that contamination is minimized.

Table 2 shows the quantitative composition results of the raw powder with mean size of 7 μm (represented by b) compared to the processed powders (represented by a), which were measured by X-ray Fluorescence (XRF). Comparative analysis shows that impurities of low melting point like Na_2O , SiO_2 and Ga_2O_3 all disappear after the induction plasma treatment. And the content of alumina has increased to 99.9080%. That is to say RF plasma

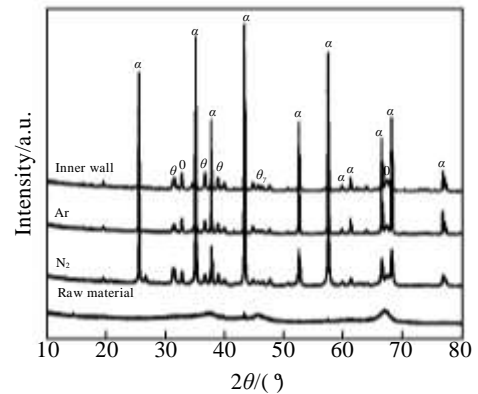


Fig.3 XRD patterns of powders before and after plasma spheroidization with different sheath gas (Ar and N_2) (28 kW, $V=65$ g/min, chamber pressure=0.079 MPa, carrier gas flow rate=5 L/min)

spheroidization is in favour of the purification of raw alumina powders in the preparation process, which is an important factor that overmatch other production methods.

2.3 Effect analysis of main operating parameters

The processed powders with mean particle size of 7 μm were discussed since it is more difficult to be synthesized. Table 3 lists different operating parameters which were used to optimize the spheroidization process. The principal factors controlling the spheroidization process of Al_2O_3 powders are the powder feeding rate, the reaction chamber pressure and their interactions with carrier gas flow rate. The injection probe position may be the most important factor because it guarantees enough energy exchange for the powder melty.

The spheroidization percentage was measured by scanning electron microscopy (SEM). 1000 processed particles were counted for each process

2.3.1 Injection probe position

Fig.4 schematically shows the position of the injection

Table 2 Quantitative result of XRF (b: initial powder particles, a: processed powder particles)

Analyte	Result (b/a)	Proc.-Calc	Line	Net Int. (b/a)	BG Int. (b/a)
Al ₂ O ₃	99.6676%/99.9080%	Quant.-FP	Al K α	144.279/135.619	5.957/5.828
Fe ₂ O ₃	0.0400%/0.0503%	Quant.-FP	Fe K α	0.179/0.210	0.071/0.065
Ga ₂ O ₃	0.0165%/0.0417%	Quant.-FP	Ga K α	0.212/0.080	0.229/0.039
Na ₂ O	0.1586%/0	Quant.-FP	Na K α	0.036	0.004
SiO ₂	0.0734%/0	Quant.-FP	Si K α	0.033	0.002
Cr ₂ O ₃	0.0440%/0	Quant.-FP	Cr K α	0.091	0.042

Table 3 Main operating parameters and spheroidization percentage

Condition No.	Z/cm	Q ₁ /Q ₂ (L min ⁻¹)	Q ₃ /L min ⁻¹	V/g min ⁻¹	P/6.89 × 10 ⁻³ MPa	Spheroidization/%
1	10.0	15(Ar)/60(Ar)	3	10	10	<10.0
2	11.0	15(Ar)/60(Ar)	5	10	11.5	<10.0
3	11.0	15(Ar)/60(N ₂)	9	10	18	<10.0
4	12.5	15(Ar)/60(Ar)	3	10	10	~96.1
5	12.5	15(Ar)/60(Ar)	9	10	10	~88.3
6	12.5	15(Ar)/60(Ar)	9	10	18	~95.3
7	12.9	15(Ar)/60(Ar)	5	65	11.5	~98.4
8	12.9	15(Ar)/60(Ar)	5	128	11.5	~83.1
9	12.9	15(Ar)/60(Ar)	5	235	11.5	~61.2
10	12.9	15(Ar)/60(Ar)	5	235	18	~53.2
11	12.9	15(Ar)/60(Ar)	9	235	18	~76.5
12	12.9	15(Ar)/60(N ₂)	5	65	11.5	~99.9
13	12.9	15(Ar)/60(N ₂)	9	65	18	~97.0
14	12.9	15(Ar)/60(N ₂)	9	235	18	~78.6

Note: The measurement and the spheroidization ratio are defined as the number percentage of spherical particles out of the total particles. Q₁, Q₂, and Q₃ represent center gas (Ar), sheath gas (Ar/N₂) and carrier gas (Ar), respectively. V represents powder feeding rate (g/min). P represents reaction chamber pressure

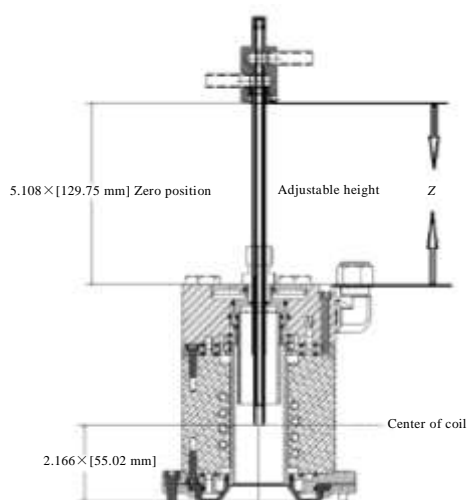


Fig.4 Position of the injection probe

probe within the induction plasma torch used in this experiment. In this work, different probe positions have been attempted. As shown in Table 3, the results of condition 1 and 4, 3 and 13 clearly reveal the influence of the probe position on the efficiency of spheroidization. Like condition 1 with Z=10 cm, there are hardly obtained spherical powders. It is because if the probe tip is too low like Z=10.0 cm, large sized powders will not get enough energy for melting, then the powders carried by argon will be sent out of the plasma torch without being spheroidized, but they keep the original state. Condition 4 with Z=12.5 cm gets an excellent result for the 96.147% spheroidization percentage. However, the spheroidization percentage reaches almost 100% when the probe position is set up to Z=12.9 cm. Condition 3 and 13 show the same result with the influence of powder feeding rate be cast aside. These results also apply to powders with mean particle size of 75 and 30 μ m.

All the results in Table 3 reveal that it is necessary to set the probe tip at the position around the middle of coil center to ensure the injected powders penetrate the plasma and get sufficient heat energy for complete melting. Then the powders are melted completely and quenched quickly; therefore, the powders get solidified with smoother surface under the action of surface tension. If the probe tip is too low, the powder particles will not get sufficient energy for melting, let alone be spheroidized. So, the injection probe position, along with the axis of the inductively coupled plasma torch, is an important operating parameter to optimize the spheroidizing treatment since it strongly influences the thermal histories of the treated particles.

2.3.2 Powder feeding rate

The influences of different powder feeding rates on spheroidization percentage have also been investigated. Condition 7, 8, 9, 13, and 14 in Table 3 suggest that the powder feeding rate strongly influences the spheroidization efficiency. Results in Fig.5 further illustrate the interactions of the powder feeding rate and carrier gas flow rate on spheroidization rate, which were calculated through the image analysis of scanning electron micrographs (SEM) of the treated powders in condition 7 (Fig.5a) and 9 (Fig.5b).

It shows that high spheroidization rate (nearly 100%) powders with smooth surface are synthesized at a proper feeding rate. However, the spheroidization rate decreases rapidly as powder feeding rate increases. That is because the amount of obtained energy per unit mass decreases when the powder feeding rate increases. The results also demonstrate that the carrier gas flow rate is another significant variable factor and strongly influences the spheroidization efficiency, as shown in Fig.5. The trends of the curve graph obviously exhibit that the excessive carrier gas flow rate is not good for spheroidization in the case of subatmospheric pressure in the reaction chamber ($0.079 \text{ MPa} < 1 \text{ atm}$).

2.3.3 Reaction chamber pressure

Reaction chamber pressure also a vitally important operating parameter during processing for it is responsible for the particle dwell time in the plasma flame. Numbers of experiments have been carried out in this work and the representative results are shown in Fig.6. The results demonstrate that the chamber pressure is also a significant factor in the spheroidization process, and it also shows there are interactions between the chamber pressure and the carrier gas flow rate. High carrier gas flow rate is not good for spheroidization with subatmospheric pressure in reaction chamber, while low carrier gas flow rate is also not good for spheroidization with positive pressure as well. Furthermore, both low and high carrier gas flow rate are not favourable for spheroidization under atmospheric pressure. Therefore, reaction chamber pressure should be coordinated with the suitable carrier gas flow rate to keep the optimal

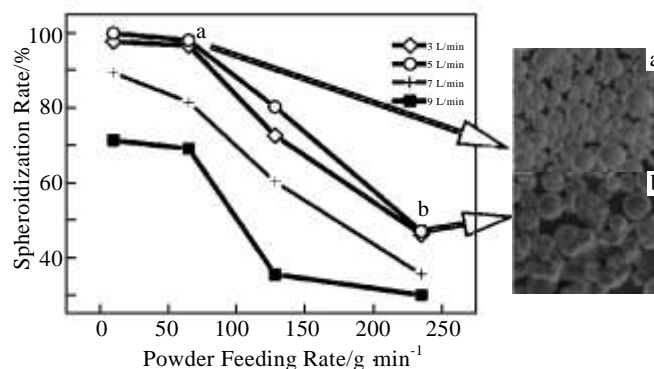


Fig.5 Interactions of the powder feeding rate and carrier gas flow rate on spheroidization rate 28 kW ($Z=12.9 \text{ cm}$, chamber pressure= 0.079 MPa)

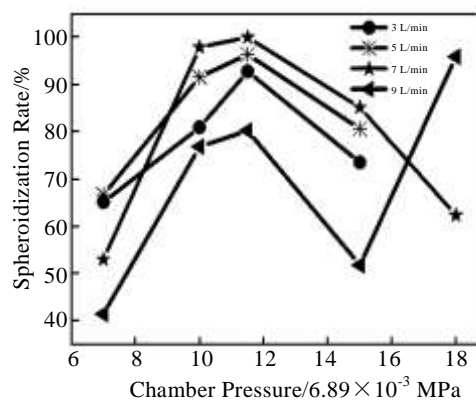


Fig.6 Interactions of reaction chamber pressure and carrier gas flow rate on spheroidization rate (28 kW, $Z=12.9 \text{ cm}$, powder feeding rate= 65 g/min)

reaction conditions between $0.026\text{--}0.079 \text{ MPa}$ in reaction chamber; otherwise the plasma flame would be quenched, as shown in Fig.6 (5 L/min and 3 L/min). These results clearly indicate that chamber pressure is so important that it requires careful selection and adjustment.

3 Conclusions

1) In this work, micro-fine spherical alumina particles with mean diameters of 7, 30 and $75 \mu\text{m}$ have been synthesized. The particle size and distribution of raw powders have a strong influence on the quality of processed particles.

2) The alumina powders are not nitrogenized by nitrogen as sheath gas during the spheroidization. The content of alumina increases to 99.9080% after RF plasma spheroidization process.

3) The probe tip position should be put in the hot core of the plasma torch with $Z=12.9 \text{ cm}$. Both argon and nitrogen can be used as the sheath gas in this work. Powder feeding

rate should be moderated like $V=65$ g/min for 30 and 75 μm and $V=35$ g/min for 7 μm . Reaction chamber pressure should be coordinated with the suitable carrier gas flow rate to keep the plasma flame on, and $P=0.079$ MPa would be the best choice for all powders.

References

- Shinoda Kentaro, Kojima Yoichi, Yoshida Toyonobu. *Journal of Thermal Spray Technology*[J], 2005, 14(4) : 511
- Heberlein Joachim, Murphy Anthony B. *Journal of Physics D: Applied Physics*[J], 2008, 41(5): 053001
- Qu Xuanhui, Sheng Yanwei, Guo Zhimeng et al. *Materials China*[J], 2011, 30(7): 10 (in Chinese)
- Pfender E. *Plasma Chemistry and Plasma Processing*[J], 1999, 19(1): 31
- Sheng Yanwei, Guo Zhimeng, Hao Junjie et al. *Procedia Engineer*[J], 2012, 36: 299
- Bai Liuyang, Fan Junmei, Hu Peng et al. *Journal of Alloys and Compounds*[J], 2009, 481: 563
- Wang Yuming, Hao Junjie, Sheng Yanwei. *Rare Metal Materials and Engineering*[J], 2013, 42(9): 1810 (in Chinese)
- Legros C, Carry C, Bowenc P et al. *Journal of the European Ceramic Society*[J], 1999, 19: 1967
- Roger B Bagwell, Gary L Messing. *Journal of the American Ceramic Society*[J], 1999, 82(4): 825
- Li J G, Ikeda M, Ye R et al. *Journal of Physics D: Applied Physics*[J], 2007, 40: 2348
- Károly Z, Szépvölgyi J, Farkas Z. *Powder Technology*[J], 2000, 110(3): 169
- Fan Yousan, University Q. *Advances in Mechanics*[J], 1990, 20(3): 67 (in Chinese)
- Marko Nagode, Frank Langler, Michael Hack. *Engineering Failure Analysis*[J], 2011, 18: 1565
- Fan X, Gitzhofer E, Boulos M. *Journal of Thermal Spray Technology*[J], 1998, 7(2): 247
- Jang Juyong, Takana Hidemasa, Park Sangkyu et al. *Journal of Thermal Spray Technology*[J], 2012, 21(5): 900
- Wang Jianjun, Hao Junjie, Guo Zhimeng et al. *Journal of the Chinese Ceramic Society*[J], 2014, 42(10): 2922
- Ye R, Ishigaki T, Jurewicz J et al. *Plasma Chemistry and Plasma Processing*[J], 2004, 24(4): 555
- Colombo V, Ghedini E, Sanibondi P. *Journal of Physics D: Applied Physics*[J], 2010, 43: 105 202
- Colombo V, Ghedini E, Sanibondi P. *Plasma Sources Science and Technology*[J], 2010, 19: 065 024

射频等离子体球化系统参数对制备球形 Al_2O_3 的影响

代 珍, 曹永革, 麻朝阳, 唐 飞, 张建涛, 王文超, 杜苗苗, 龙嘉奇, 袁轩一
(中国人民大学 北京市光电功能材料与微纳器件北京市重点实验室, 北京 100872)

摘 要: 以不规则 Al_2O_3 粉体为原料, 采用TEKNA射频感应等离子体球化设备SY119-30kW制备不同粒度的(7, 30, 75 μm)微细球形 Al_2O_3 粉体, 并研究了主要操作参数的影响。结果表明不同的探针轴向位置对球化效果有较大的影响, 必须保证针尖在等离子体中心位置, 即 $Z=12.9$ cm。等离子球化工艺制备的 Al_2O_3 粉体不仅表面光滑, 而且球形度高, 致密度高, 流动性好。在反应腔体压力为负压 $P=0.079$ MPa的情况下, 送分速率为65 g/min时, 粉体球化率可以达到100%; 反应腔室的压力对球化效果的影响较大, 其必须与载气流量保持协调。经XRD物相分析可知, 分别采用Ar或者 N_2 为鞘气都可以得到相同的物质组成, 高温下 N_2 并没有使 Al_2O_3 氮化。同时, 等离子体球化具有提纯的作用, 球化后的粉体纯度得到改善。

作者简介: 代 珍, 女, 1988年生, 硕士, 中国人民大学光电功能材料与微纳器件北京市重点实验室, 北京 100872, 电话: 010-82502773, E-mail: daizhenzhendaizhen@163.com